CHAPTER 5
MODAL IDENTIFICATION

5.1 Modal Analysis

The response of a cylinder under external load can be described conveniently by using modal analysis. The method is intended to express the response as a superposition of the system's eigenfunctions multiplied by their corresponding time-dependent natural coordinates. As an illustration of this method, consider a uniform string under tensile load with pinned end boundary conditions. The equation of motion for this boundary value problem is:

$$Ty''(X,t) - R(X)\dot{y}(X,t) + f(X,t) = m(x)\ddot{y}(X_1 t) \qquad (5.1.1)$$

The response y(x,t) may be expressed as a superposition of normal mode responses.

$$Y(X,t) = \sum_{r=1}^{\infty} Y_r(X)P_r(t) \qquad (5.1.2)$$

where Yr(x) is the normalized mode shape and has the following orthogonality property.

$$\int_0^{\ell} m(x)\ Y_r(x)Y_s(x)\ dx = \delta_{rs} \qquad (5.1.3)$$

Substitution of (5.1.2) into (5.1.1) multiplication by Ys(x), and integration from x=0 to L leads to:

$$\ddot{P}_r(t) + \dot{P}_r(t)\int_0^{\ell} R(x)Y_r(x)Y_s(x)dx + w_r^2 P_r(t) = N_r(t) \qquad (5.1.4)$$

If R(x) is proportional to m(x), orthogonality of normal modes leads to a set of uncoupled single degree of freedom oscillation equations in terms of the natural coordinates Pr(t).

For $R(x) = C\ m(x)$ (5.1.5)

$$\ddot{P}_r(t) + c\dot{P}_r(t) + w_r^2 P_r(t) = N_r(t) \qquad (5.1.6)$$

where Nr(t) the modal force defined as:

$$N_r(t) = \int_o^{\ell} Y_r(x)\ f(x,t)\,dx \qquad (5.1.7)$$

In reality, the damping may not be governed by equation 5.1.5. However, for lightly damped well separated modes, the uncoupled assumption yields good results. Such is the case here. By an analogous derivation, the uncoupled normal mode equations may be derived for a beam under tension, with pinned end conditions. For a uniform beam the mode shapes are sinusoids as they are for a uniform string. By using modal analysis, the continuous system is reduced to many single degree of freedom systems. In the next section we will estimate the natural coordinate time histories, $P_r(t)$, from measured responses at the accelerometer locations.

5.2 Estimation of Natural Coordinates

In the preceding section, the response of the cylinder was expressed in terms of a superposition of mode shapes $Y_r(x)$ multiplied by the natural coordinates $P_r(t)$:

$$y(X,t) = \sum_{r=1}^{\infty} P_r(t)\ Y_r(x) \qquad (5.2.1)$$

In this experiment, the response was measured at seven positions. They are at 1/8L, 1/6L,1/4L,2/5L,1/2L,5/8L,3/4L. In this study a least squares method was used to estimate the natural coordinates in terms of the measured responses at these seven positions. For any test case the response is dominated by a finite number of modes usually 2 to 6 in number. A first guess at the responding modes may be obtained by inspection of the response spectrum at any one location. By summing the normal mode responses over the apparent participating modes, the following equations are obtained, where the range M~N covers all of the participating modes. The mode shapes can be calculated theoretically. For the pin-supported uniform cylinder, the mode shapes are given by

$$Yr(x)=\sin(r\pi x/L)$$

At time t=to, the response of position $x=X_j$ can be expressed as:

$$Y(X_j,t_o) = \sum_{i=m}^{N} P_i(t_o)Y_i(X_j) + E(X_j) \qquad (5.2.2)$$

where $E(X_j)$ is the noise term.

Rewriting (5.2.2) in matrix form:

$$\{y\} = [Y]\ \{P\} + \{E\} \qquad (5.2.3)$$

where y_j is the vector of the measured response

Y_{ij} is the mode shape matrix

P_i is the vector of the natural coordinate

E_j is the vector of noise (or error)

$i=m,N \quad j=1,7$

The sum of error squares ee is given by

$$ee = \langle E \rangle \{E\} = \{\{y\} - [Y]\{P\}\}^T\{\{y\}-[Y]\{P\}\}$$

$$= \{y\}^T\{y\}- 2\{P\}^T[Y]^T\{y\} + \{P\}^T[Y]^T[y]\{P\} \qquad (5.2.4)$$

The vector of natural coordinates Pi is to be determined such that the error squared term is minimized.

$$\min[ee] = \min[\{E\}^T\{E\}]$$

Let

$$\frac{d}{dP_i}(ee) = 0 \qquad (5.2.5)$$

and solve for P(t).

$$\{P\} = [[Y]^T[Y]]^{-1}[Y]^{-1}\{y\} \qquad (5.2.6)$$

or

$$\{P\} = [T]\ \{y\} \qquad (5.2.7)$$

where [T] is the transfer matrix:

$$[T] = [[Y]^T[Y]]^{-1}[Y]^T \qquad (5.2.8)$$

Equation (5.2.7), decomposes the measured response at the seven positions into the natural coordinates provided the mode shapes are known and the guess of the responding modes is initially correct. Figure 22 showed an example of the horizontal pipe vibration displacement at position L/8. It is clear that several modes were excited. In the displacement spectrum, there are several peaks, each corresponding to one particular mode to be identified. Using the method discussed above, the natural coordinate time histories were obtained for the 4th, 5th, 6th and 7th modes corresponding to each peak in the displacement spectrum, shown in Fig. 23. These natural coordinate time histories are shown in Fig. 29. The FFT of fourth- and fifth-mode natural coordinates are shown in Figs. 30 and 31. Each natural coordinate time history represents the antinode displacement for that mode. Their sum does not equal the displacement portrayed in Fig. 22 because it is the motion at a specific point on the cable.

5.3 Response Mode of In-line Motion at Lock-in

In Chapter 4 it was stated that at lock-in the in-line response is at twice the frequency of the cross-flow. The question arises, what mode responds in the in-line direction. These modal identification techniques have been used to provide the answer, with some very surprising results. One

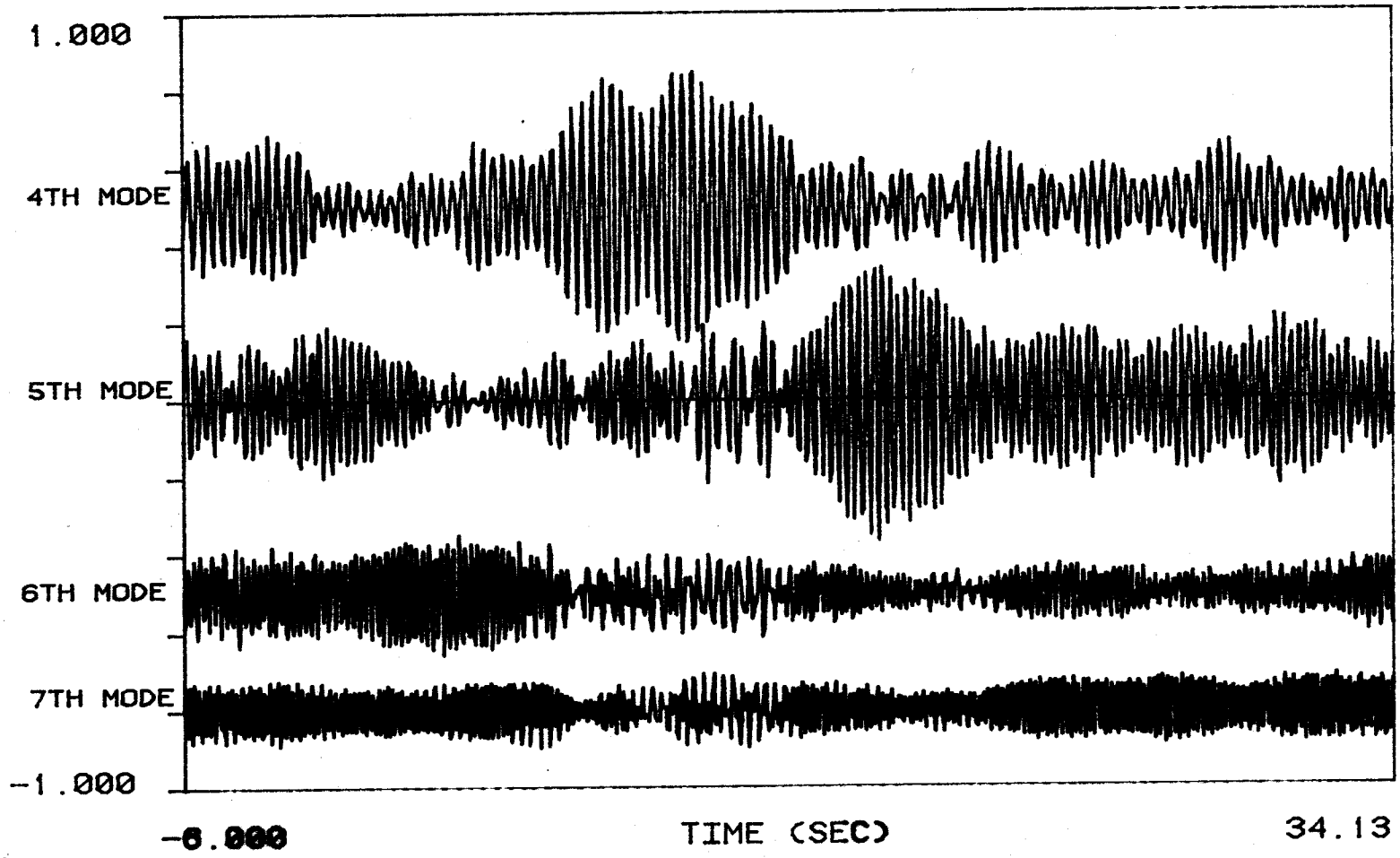

FIG.29 NATURAL COORDINATE TIME HISTORIES FOR THE 4TH, 5TH. 6TH. AND 7TH MODES OF THE PIPE

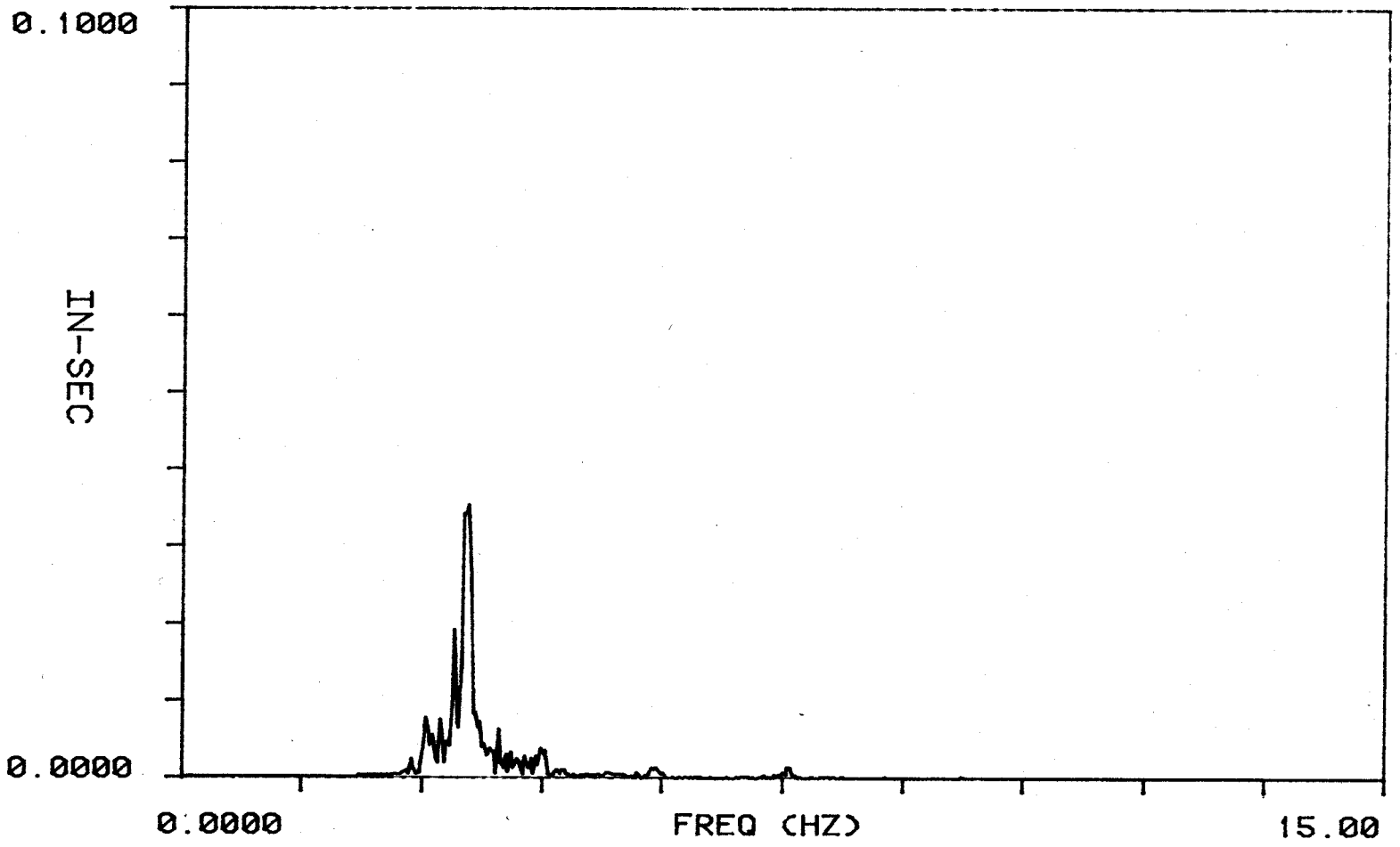

FIG.30 FFT OF THE 4TH NATURAL COORDINATE TIME HISTORY

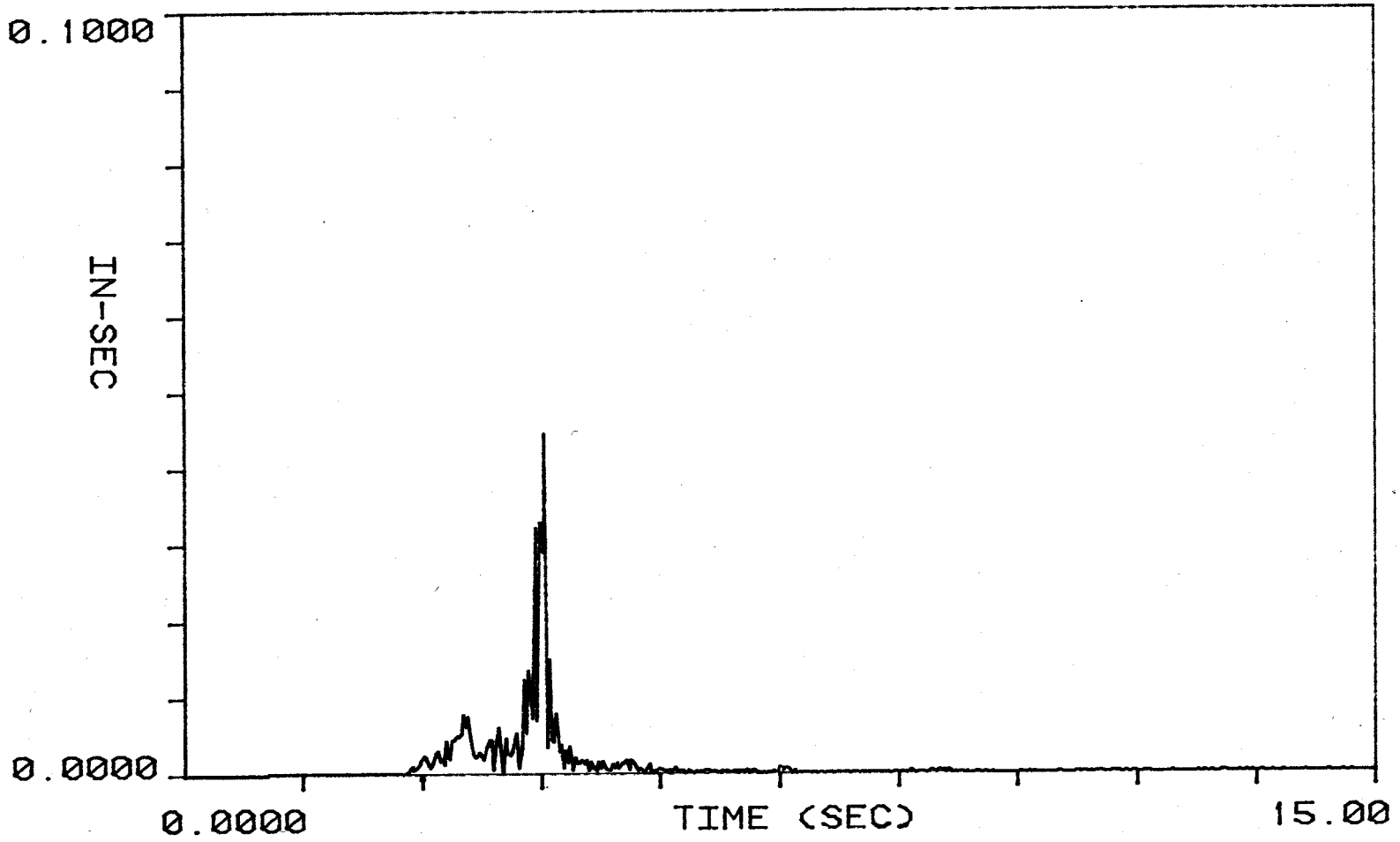

FIG.31 FFT OF THE 5TH NATURAL COORDINATE TIME HISTORY

such interesting case as described below.

For a taut cable,all of the natural frequencies are integer multiples of the lowest. Therefore it is reasonable to expect that the fluctuating drag forces will excite an in-line mode whose natural frequency is twice that of the mode which is responsible for the cross-flow lock-in. As will be shown, this is often not the case. Figures 32 through 35 are the displacements and FFT's of the cable in the vertical and horizontal directions at L/8. The cross-flow motion is at the second-mode natural frequency of the cable, and the in-line motion is at the fourth-mode natural frequency. Least squares modal identification was carried out in both directions and the resulting natural coordinates revealed that the vertical vibration was in the second-mode shape, while the horizontal vibration was in the third-mode shape instead of the fourth-mode as had been expected. The frequency of this third mode motion was not the natural frequency of the third mode but was in fact equal to the natural frequency of the fourth mode. The response was not resonant, but inertia controlled response of the third mode. Why was there no resonant response in the fourth mode? A close look at the fluctuating drag forces provides the explanation. For all pin-ended, uniform cylinders in a uniform flow, lock-in with cross-flow vibration modes generates fluctuating drag forces which are symmetrically distributed about the center of the cylinder. The resulting modal exciting forces are given by equation 5.1.7. If a mode

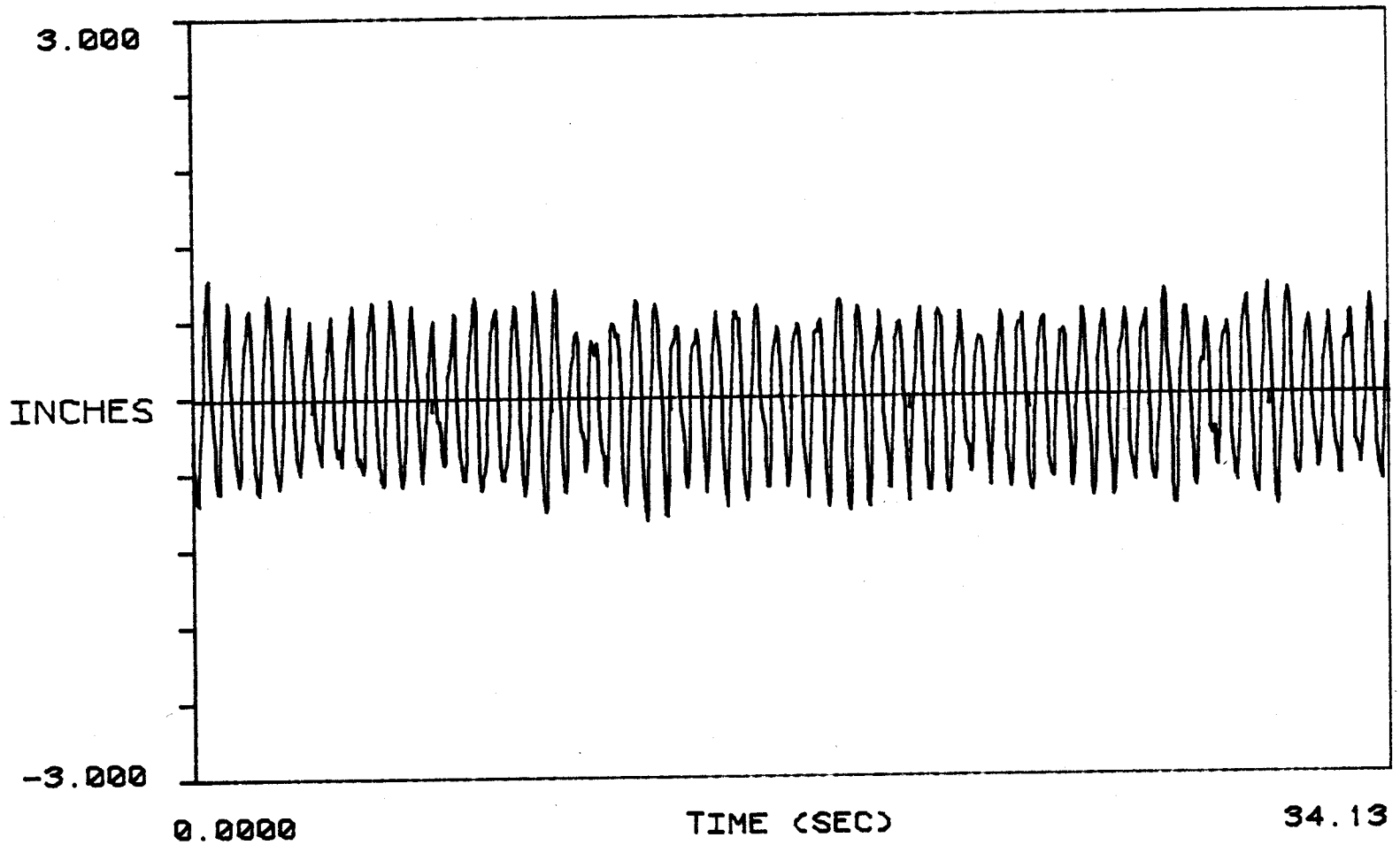

FIG.32 CROSS-FLOW DISPLACEMENT OF THE CABLE AT L/8

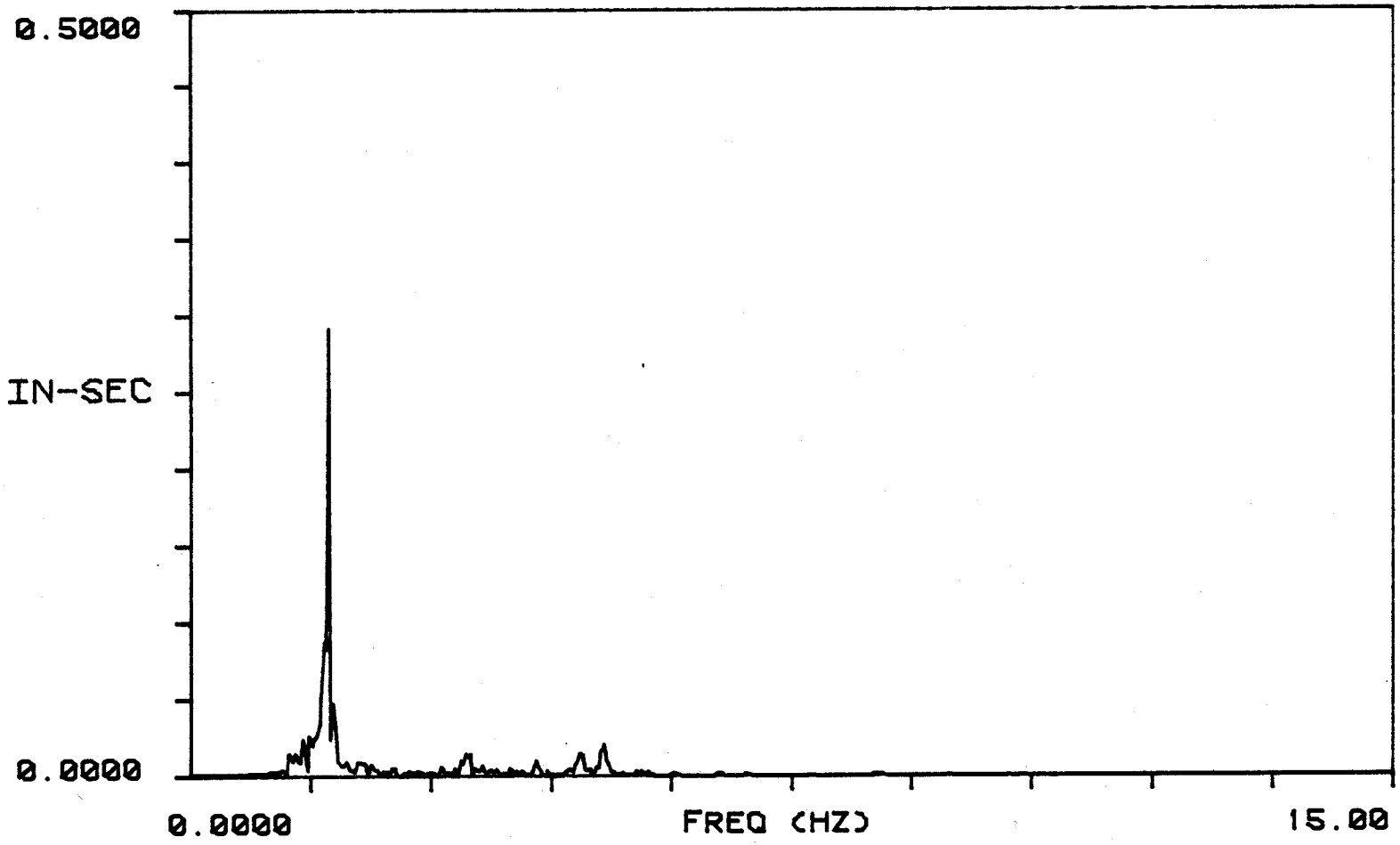

FIG.33 FFT OF THE CROSS-FLOW DISPLACEMENT IN FIG.32

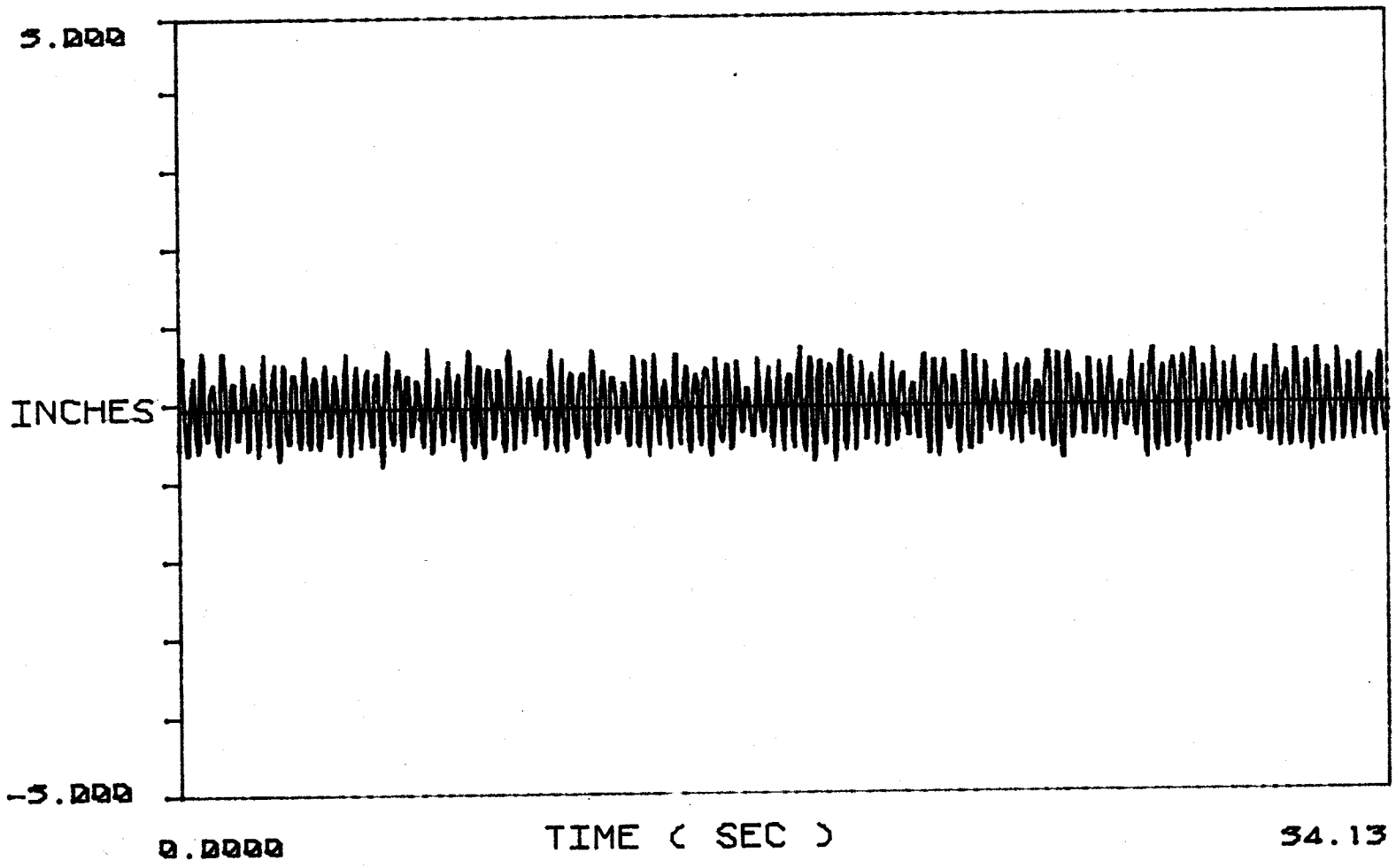

FIG.34 IN-LINE DISPLACEMENT OF THE CABLE AT L/8

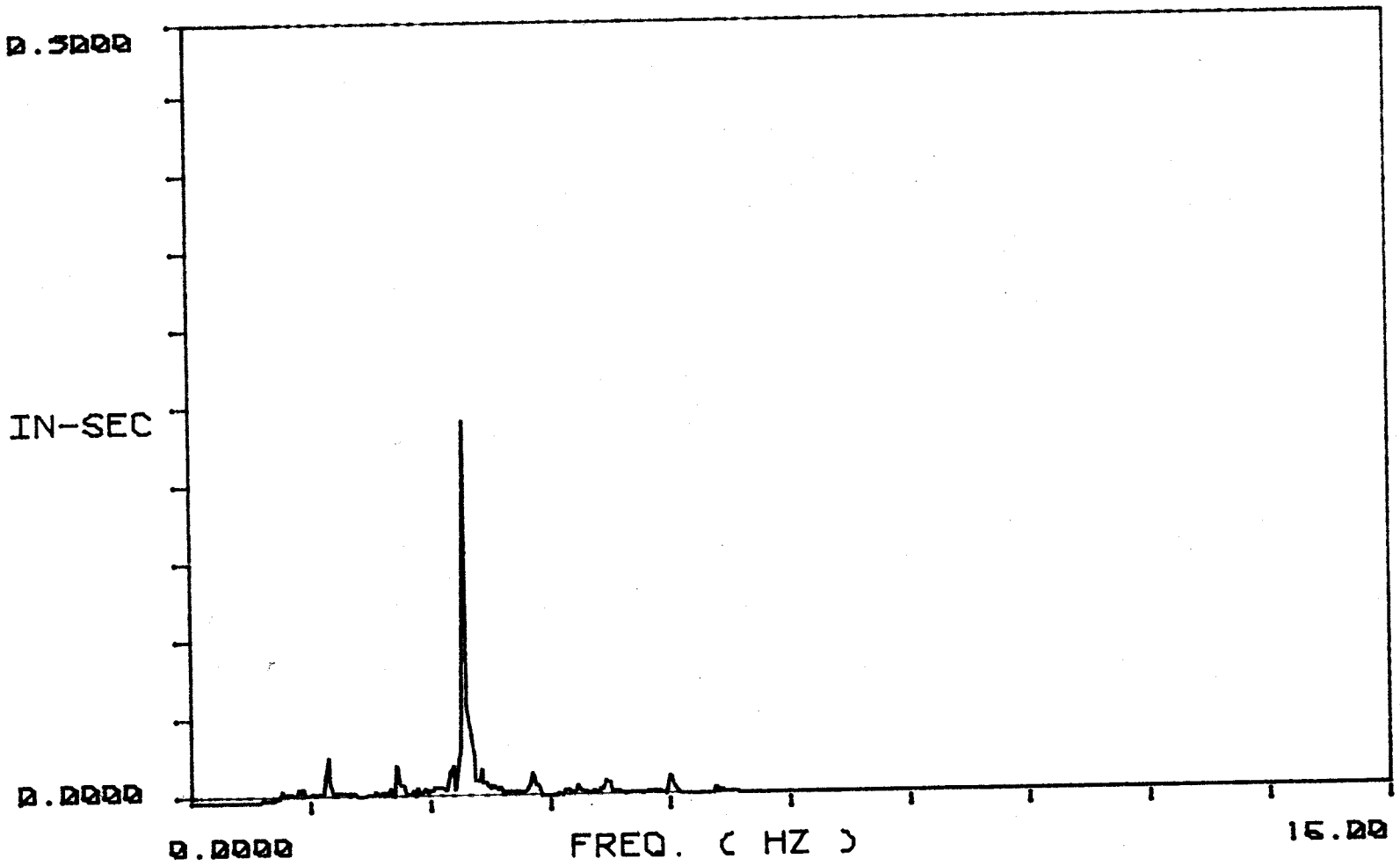

FIG.35 FFT OF THE IN-LINE DISPLACEMENT IN FIG.34

shape is asymmetric with respect to the center of the cylinder, this integral and hence the modal force are zero. If the mode shape is a symmetric function with respect to the center, the integral and resulting modal force are non-zero. For cables and pipes under tension with pinned ends, the even-numbered modes are asymmetric and, hence, cannot be excited. The odd-numbered modes are symmetric with respect to the center and may be excited. In this particular case, even though the excitation was near the natural frequency of the fourth in-line mode, the modal force of the fourth mode was zero. The observed response was principally in the third mode. Figure 36 shows the natural coordinates of different modal participations in displacement in the horizontal direction.

5.4 RMS Response in the Natural Coordinates During Non-lock-in

Lock-in responses can be described by periodic deterministic models. Non-lock-in has a much more random character. At constant current speed and non-lock-in conditions, the participation of the contributing modes varies with time. An example of this spanning a very short period of time was presented in Fig. 29, in the section on modal coordinate identification. It is enlightening to study non-lock-in response on a longer time scale. A 448-second record of non-lock-in pipe response was analyzed and the natural coordinate contributions were separated by the methods described previously. Moving average RMS natural

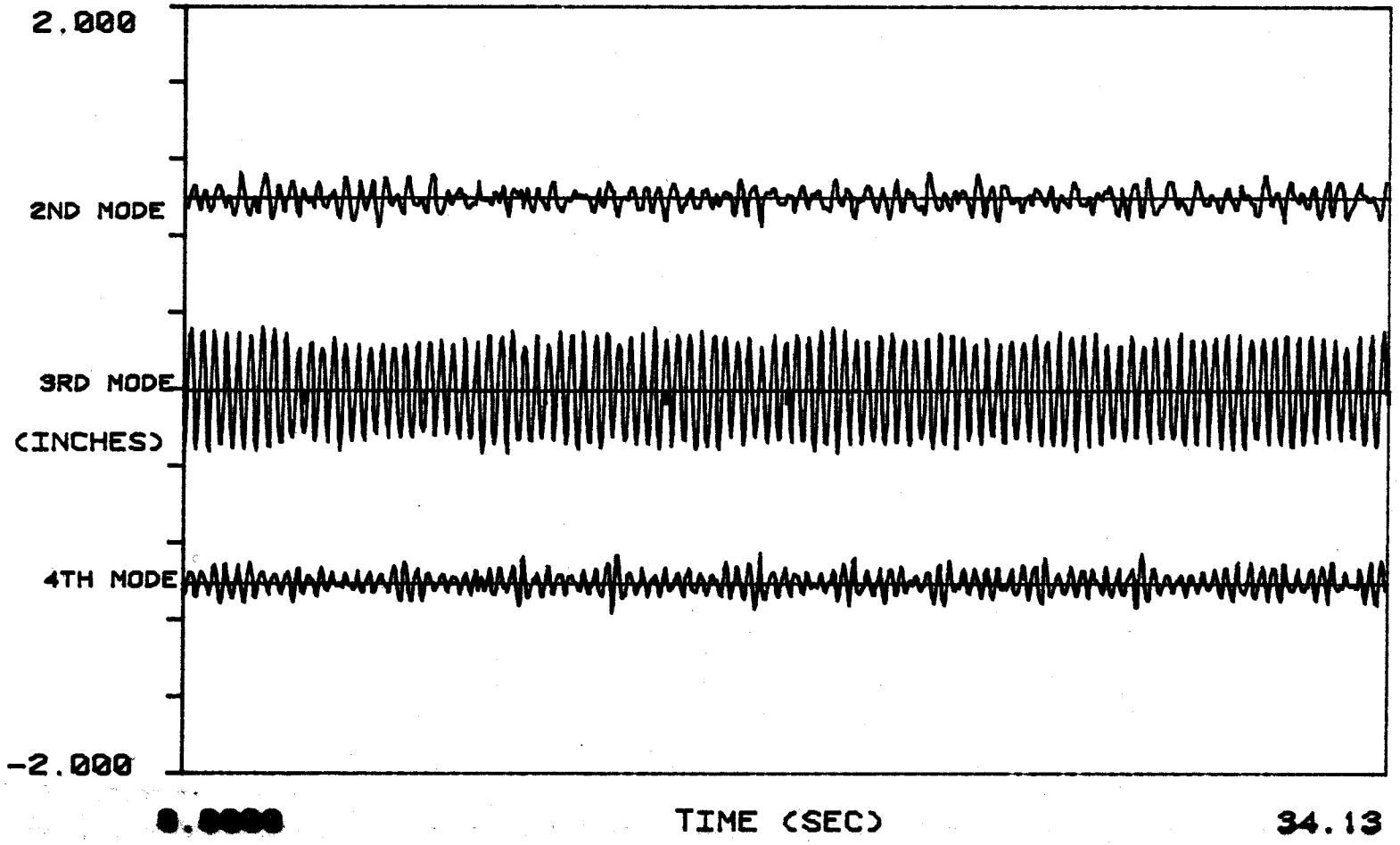

FIG.36 IN-LINE NATURAL COORDINATE TIME HISTORIES FOR 2ND. 3RD. AND 4TH MODES OF THE CABLE

coordinate responses were calculated. These are plotted in Figs. 37 and 38. These responses reflect the RMS values of the individual modal anti-node responses. The current and drag coefficient for the same time interval is shown in Fig. 39. The total response stays approximately constant while the individual modal contributions vary over wide ranges. As one mode recedes, another appears to take its place.

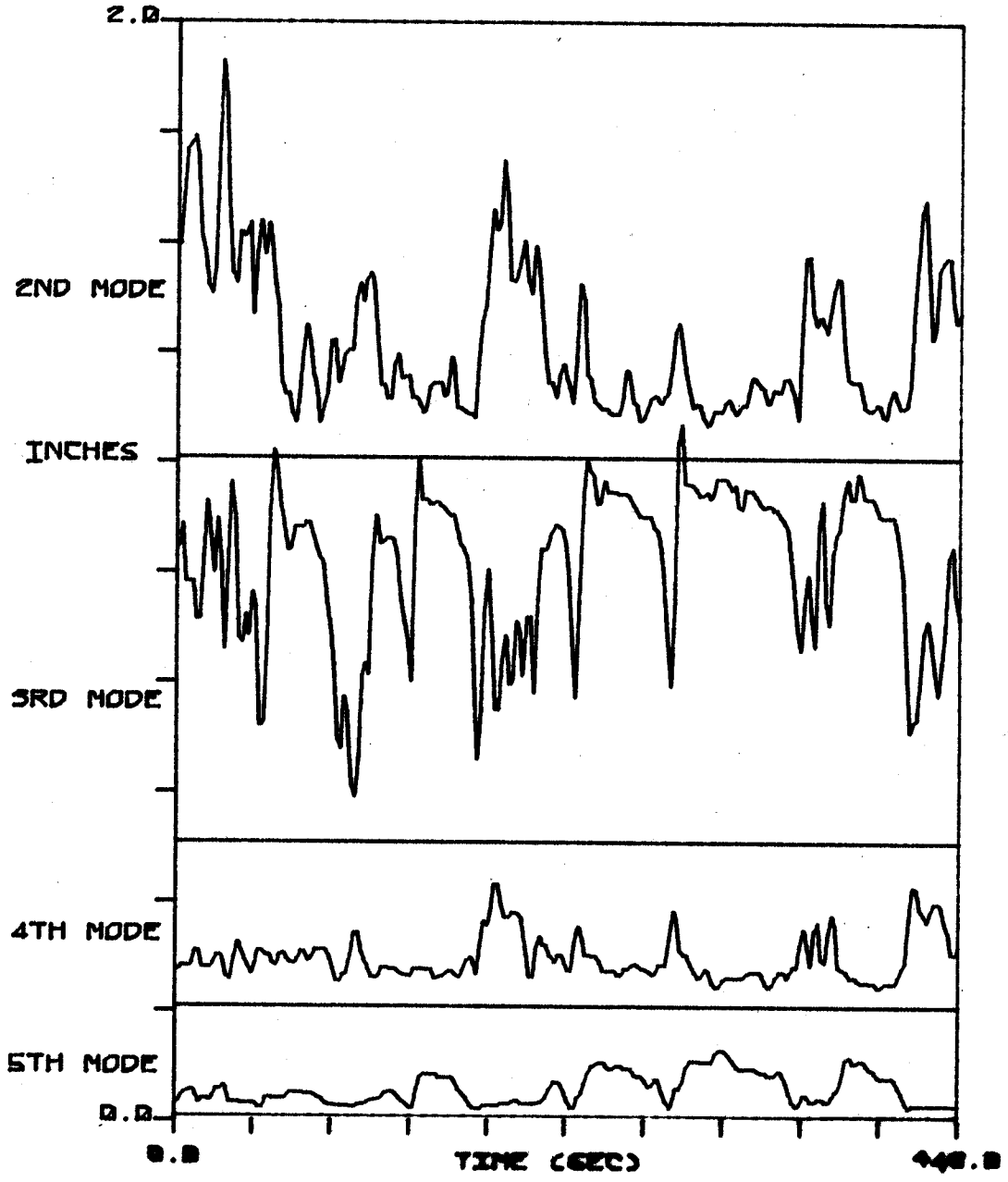

FIG.37 RMS OF THE NATURAL COORDINATES FOR THE 2ND, 3RD, 4TH AND 5TH CROSS-FLOW MODES OF THE PIPE

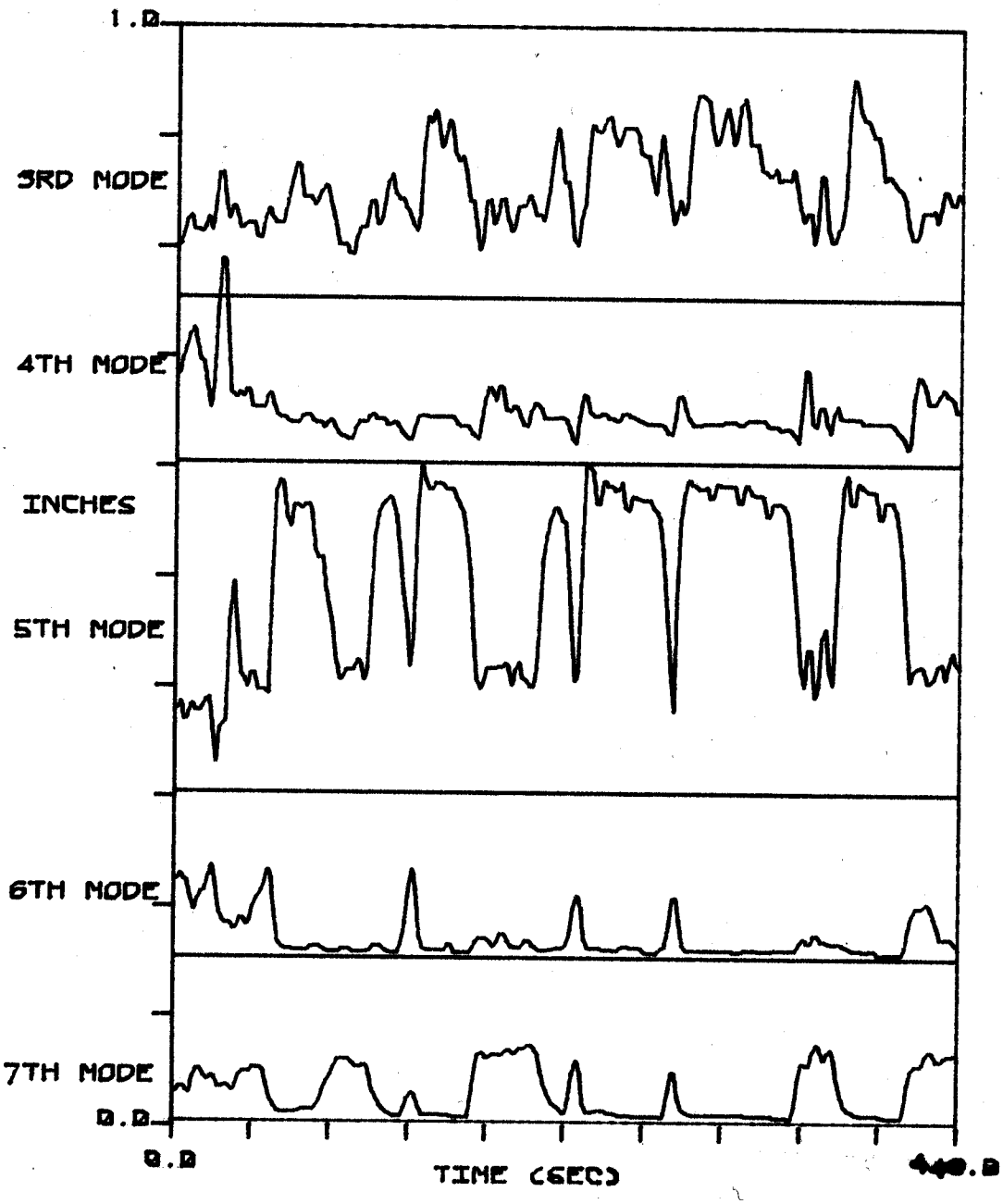

FIG.38 RMS OF THE NATURAL COORDINATES FOR 3RD, 4TH, 5TH, 6TH AND 7TH IN-LINE MODES OF THE PIPE

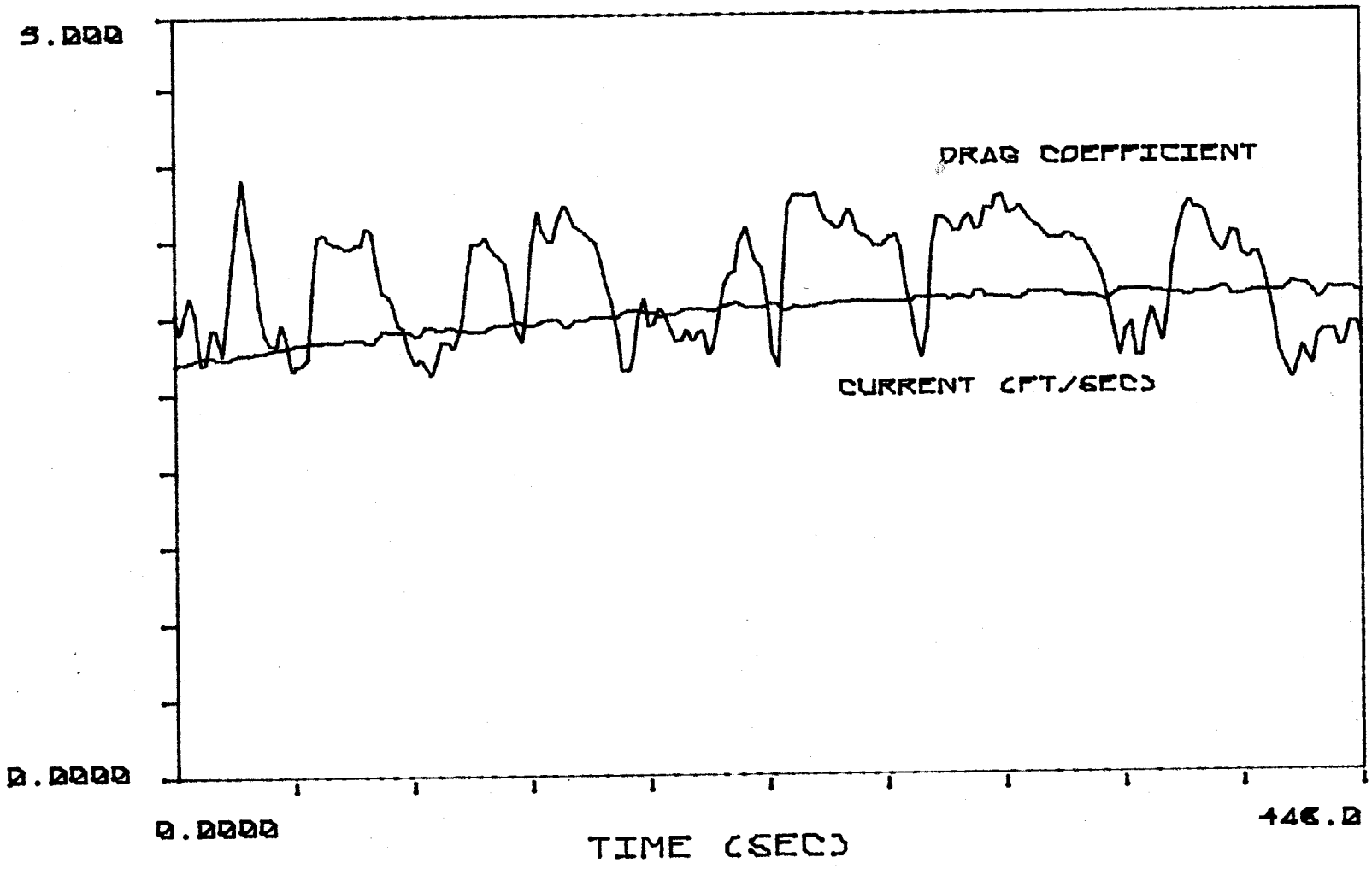

FIG.39 DRAG COEFFICIENT AND CURRENT
CORRESPONDING TO FIG.37 AND 38

CHAPTER 6

CONCLUSION

The following conclusions may be made based on the test data presented:

i. At lock-in, the transverse motion is characterized by single-mode response. The in-line motion may have two modes: the dominant one has a frequency twice that of the transverse frequency and need not be the resonant response of any particular mode, the smaller in-line response component is at the frequency of the cross flow vibration and represents a small amount of resonant in-line vibration which is driven by unknown coupling mechanisms to the cross flow vibrations. Motion time histories at lock-in are deterministic. The phase between the in-line and cross-flow components occasionally results in figure 8 patterns (as in Fig. 19). Many other repeating patterns have been observed, depending on the position on the cable and the principal responding mode. The amplitude of transverse response is about twice that of the in-line motion. A narrow band periodic lift force is implied.

ii. At lock-in, the in-line response is at twice the frequency of the transverse motion. The responding in-line mode shapes are symmetric with respect to the center of the cylinder. Asymmetric modes are excited very little due to the symmetric distribution of the drag exciting forces.

iii. At non-lock-in, several modes respond in both in-line and transverse directions, and the center frequency of the in-line motion is higher than that of the transverse. Wide-band lift and drag forces are implied.

iv. At non-lock-in ,vibration energy can transfer from one mode to another mode without any significant change in current speed as shown in Fig. 29.

v. Maximun drag coefficient occurs at lock-in, and is about 3.0 for the pipe, and 3.3 for the bare cable as shown in the 2 1/2-hour RMS data. Maximum RMS transverse and in-line displacements also occur at lock-in. However, peak responses are usually higher in the non-lock-in motion.

REFERENCES

1. Basili, M. and Brady A.G. "Low Frequency Filtering and The Selection of Limits for Accelerogram Coefficients", Proc. of the Sixth European Conference on Earthquake Engineering, Yugoslavia, 1978.

2. Bendat,J.S. and Piersol, A.G., Random Data: Analysis and Measurement Procedures, John Wiley and Sons, New York, 1971.

3. Blevins, R.D., Formulas for Natural Frequency and Mode Shape, Van Nostrand Reinhold Company, New York, 1979.

4. Clough, Ray W. and Penzien, Joseph, Dynamics of Structure, McGraw-Hill, New York, 1975.

5. Gray, A.H., and Markel J.D. "A Computer Program for Designing Digital Elliptic Filters", IEEE Trans. on Acoustics, Speech, and Signal Processing, December 1976.

6. Hamming R.W., Numerical Methods for Scientists and Engineers, McGraw-Hill Co. New York, 1962.

7. King, R., "A Reveiw of Vortex Shedding Research and Its Application", Ocean Engineering, New England Section, Sept. 26, 1975.

8. McGlothlin J.C. "Drag Coefficients of Long Flexible Cylinders Subject to Vortex Induced Oscillation", Thesis Presented to the Massachusetts Institute of Technology, Cambridge, Mass. 1981.

9. Meirovitch, Leonard, Analytic Method in Vibrations, MacMillan Co., New York, 1967.

10. Oppenheim, A.V. and Schafre R.R., Digital Signal Processing, Prentice-Hall, Inc., Englewood Cliffs, N.J. 1975.

11. Rabiner, L.R. and Gold B., Theory and Application of Digital Signal Processing, Prentice-Hall, Inc. Englewood Cliffs, N.J. 1975.

12. Sarpakaya, T., "Vortex Induced Oscillations. A Selective Review." ASME Journal of Applied Mechanics, Vol. 46, June 1979, pp. 241.

13. Schuessler, H,W. and Ibler, W. "Digital Filters for Integration", European Conference on Circuit Theory and Design, Institute of Electrical Engineers, Conference Publication No. 116, 1974.

14. Skop, R.A., Griffin, O.M. and Ramberg, S.E ., "Strumming Predictions for the SEACON II Experimental Mooring," Proc. Offshore Tech. Conf., Houston, Texas, OTC 2884, 1977.

15. Trifunac, M.D. and Lee V.W. "Uniformly Processed Strong Earthquake Ground Accelerations in the Western United States of America for the Period from 1933 to 1971: Corrected Acceleration, Velocity and Displacement Curve", Report No. 78-01 Dept. of Civil Eng., U. of S. California, CA.

16. Vandiver J.K. and Griffin O.M. "Measurement of the Vortex Excited Strumming Vibrations of Marine Cables," Proc. of Ocean Structural Dynamics, 1982.

17. Vandiver J.K. "Natural Frequency, Mode Shape, and Damping Ratios for Cylinders Tested at Castine," unpublished M.I.T. Ocean Engineering Report.

18. Vandiver J.K. and Mazel, C.H. , "A Field Study of Vortex-Excited Vibrations of Marine Cable", Offshore Tech. Conf., Houston, Texas, OTC 2491, 1976.

APPENDIX 1
CASE STUDY

A case study for double integrating an acceleration time series is described here:

(1) Fig. A.1 shows the acceleration time histories to be double integrated.

(2) The first step is to obtain the theoretical FFT of diaplacement and then determine the stop-band and pass-band edge frequencies Fig. A.2 shows the theoretical FFT of displacement, from which we have:

Ws = 1.7 Hz

Wp = 2.0 Hz

(3) Determine the pass-band and stop-band ripple tolerance Ps and Pp. A typical value for Ps and Pp in the data processing presented here are:

Ps=0.01

Pp=0.01

(4) Determine the order of the filter N from design charts (10). For this case study:

N=8

(5) Calculate the positions of poles and zeros and the cascade form filter coefficients from the computer program IIR. The following parameters are obtained for the high-pass filter.

pole locations:

0.905654 + i 0.397566

0.862657 + i 0.407297

0.739515 + i 0.425226

0.419697 + i 0.286726

zero locations:

0.938481 + i 0.345329

0.948841 + i 0.315753

0.971191 + i 0.924658

(6) Carry out all eleven steps described in section 3.5 in the computer program LLITG, and the final displacement are obtained as shown in Fig. A.3 and Fig. A.4.

The programs IIR and LLITG are interactive in nature and begin with a series of queries which must be responded to by the user in order to proceed with the program. Pages 78 and 79 give the queries and the answers as used in the example in this appendix. Pages 80 and 81 give additional explanation regarding the information required in response to each of the queries. With this report, the example in the appendix and a listing of the programs the reader should be able to assemble a set of programs for the double integration of time series data. Program listings will be provided on request.

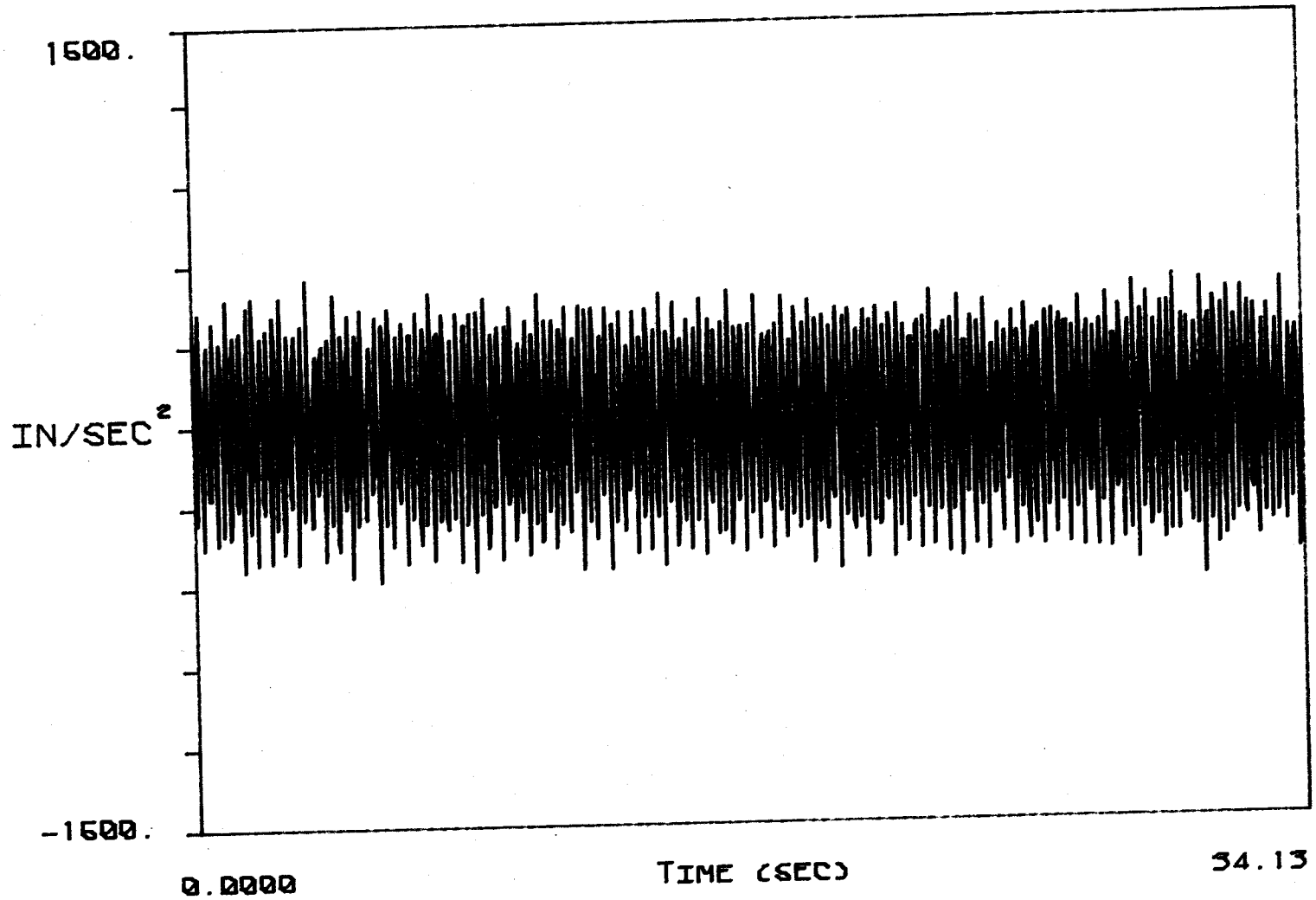

FIG. A1 ACCELERATION TIME HISTORY

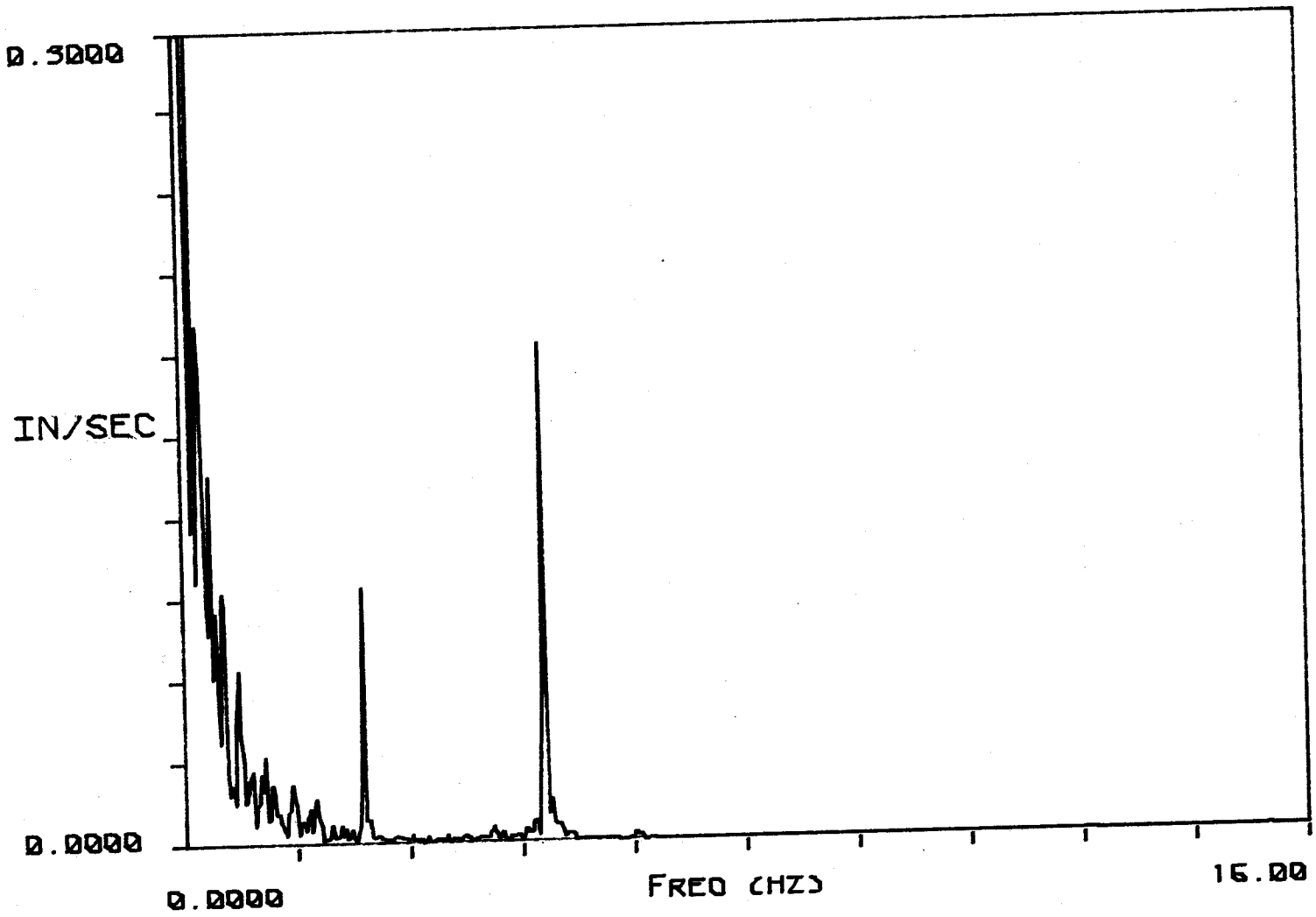

FIG. A2 THEORETICAL FFT OF THE DISPLACEMENT

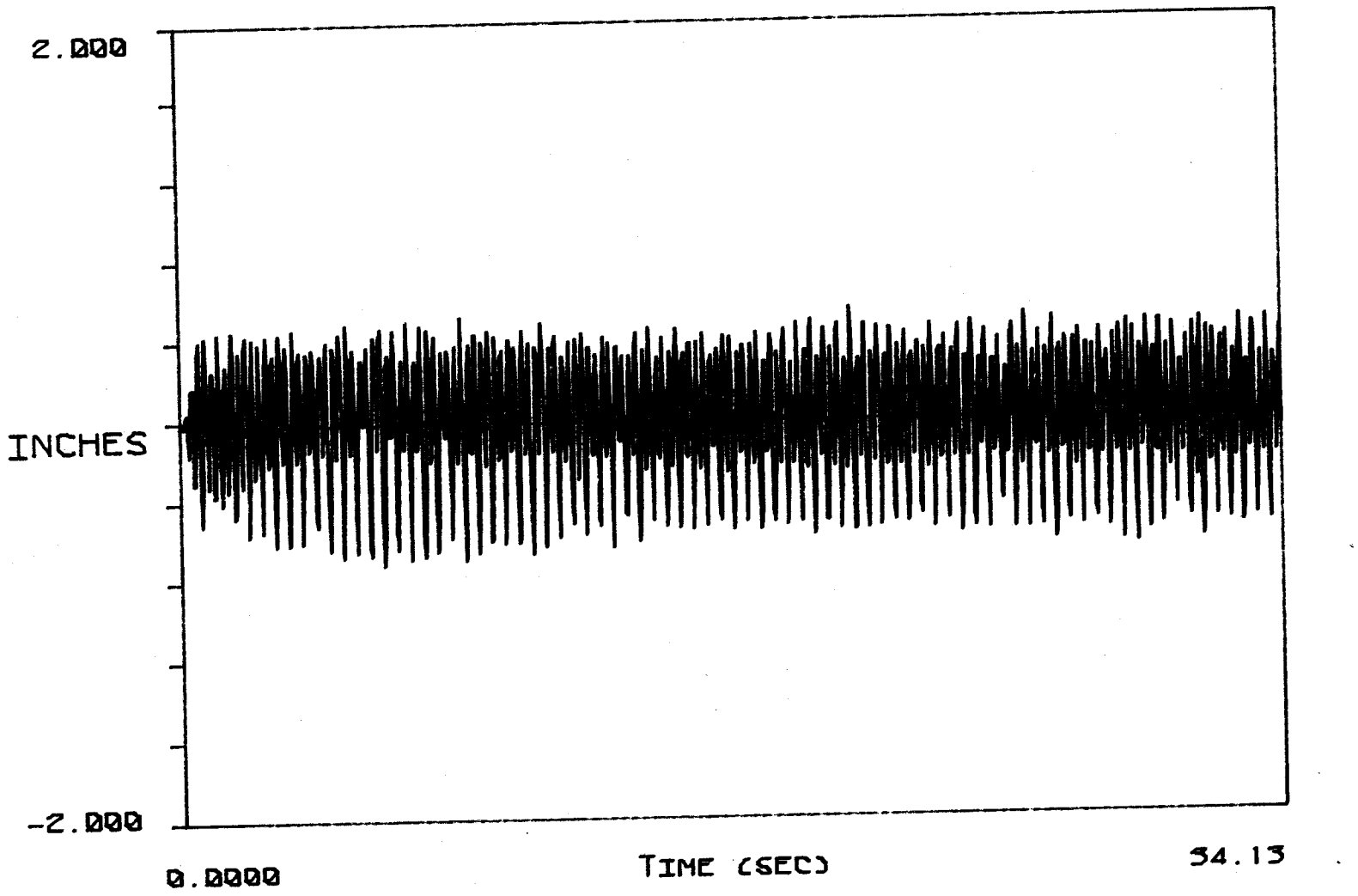

FIG. A3 DOUBLE-INTEGRATED DISPLACEMENT TIME HISTORY

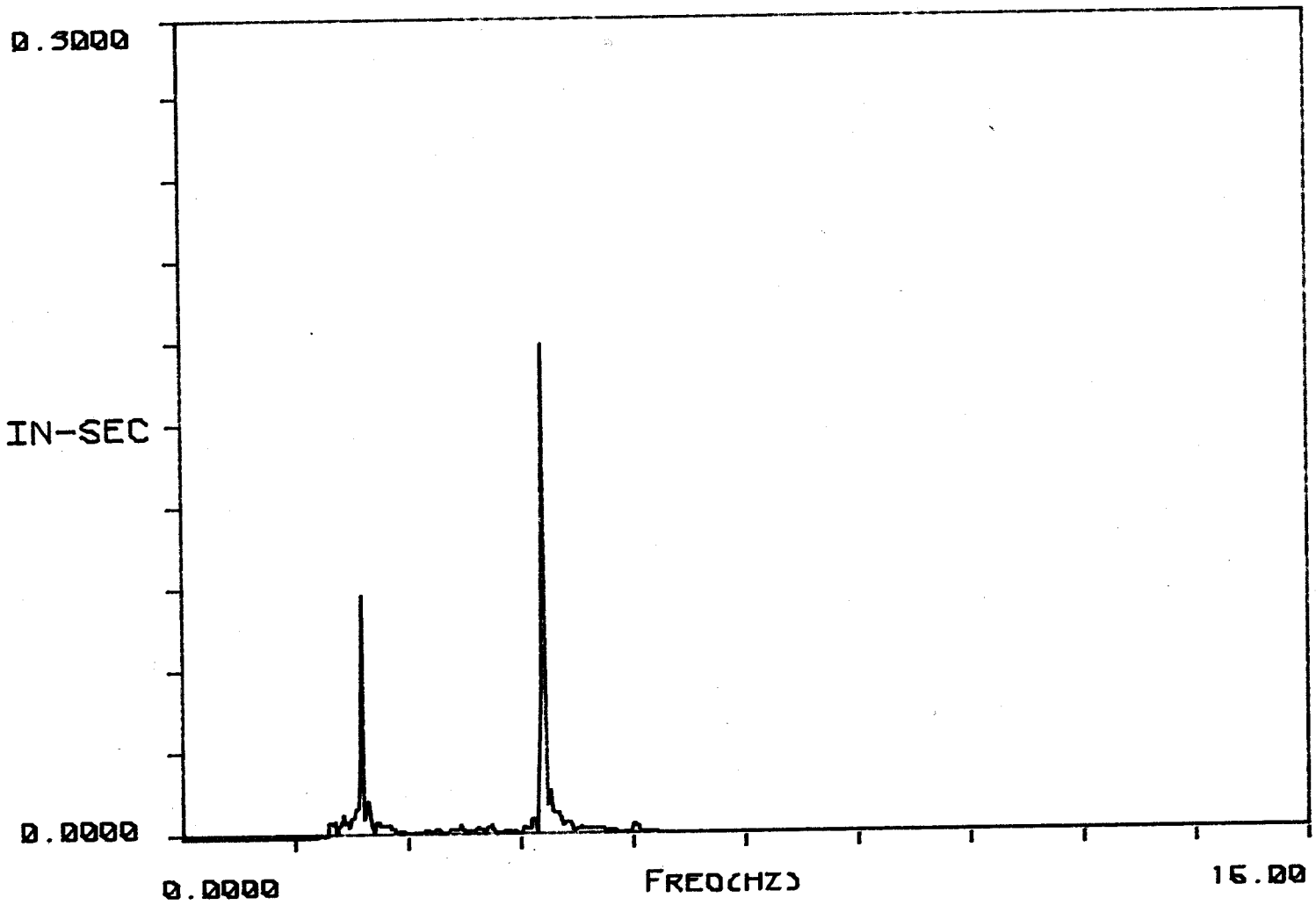

FIG. A4 FFT OF THE DOUBLE-INTEGRATED DISPLACEMENT

```
(1)  PROGRAM IIR

RUN IIR
1.   ENTER OUTPUT FILTER COEFFICIENT FILE NAME
     ?FILTER.DAT

2.   ENTER ORDER OF THE FILTER(EVEN #)
     ?8

3.   ENTER 0 FOR LOW AND HIGH PASS FILTER
     OR ENTER 1 FOR BAND PASS AND REJECT FILTER
     ?0

4.   ENTER PASS BAND RIPPLE ATTENUATION W.R.T. 1
     ?0.01

5.   ENTER SAMPLING FREQUENCY IN HZ
     30 HZ FOR CASTINE EXPERIMENT
     ?30

6.   FOR LOWPASS   : ENTER 0
     FOR HIGHPASS : ENTER PASSBAND FREQUENCY IN HZ
     FOR BANDPASS : ENTER FIRST  PASSBAND FREQ IN HZ
     FOR BANDSTOP : ENTER SECOND PASSBAND FREQ IN HZ
     ?2.0

7.   FOR LOWPASS   : ENTER PASSBAND FREQ IN HZ
     FOR HIGHPASS : ENTER SAMPLING FREQ IN HZ
     FOR BANDPASS : ENTER SECOND PASSBAND FREQ IN HZ
     FOR BANDSTOP : ENTER FIRST  PASSBAND FREQ IN HZ
     ?30

8.   FOR LOWPASS OR HIGHPASS: ENTER POSITIVE STOPBAND FREQ
     OR ENTER NEGATIVE STOPBAND RIPPLE IN DB
  ********************
```

```
FOR BANDPASS AND STOP : ENTER NEGATIVE STOPBAND RIPPLE IN DB
?1.7



(2) PROGRAM LLITG
RUN LLITG

1.   ENTER FILTER COEFFICIENTS FILE NAME
     ?FILTER.DAT

2.   ENTER # OF DATA POINTS
     ?1024

3.   ENTER SAMPLING FREQ(SAMPLES/SEC)
     ?30

4.   ENTER RAW DATA FILE NAME (BINARY DATA)
     ?C8031.RO3

5.   ENTER OUTPUT DISPLACEMENT FILE NAME (BINARY DATA)
     ?C8031.DO3
```

Description of the Program Input/Output Requirements

PROGRAM IIR:

1. FILTER.DAT is the output ASCII data file contaiing filter coefficients which is the input file to program LLITG.
2. Order of the filter which is discussed in Appendix 1-(4) in this example 8.
3. Choose correct one - 0 in this example for highpass filter.
4. e.g., for highpass filter in Figure 12, is the passband ripple expressed as a decimal fraction less than 1.0 -0.01 in this example.
5. Sampling frequency in Hz = number of samples per second - 30 Hz in this example.
6. In the example for a highpass filter as in Figure 12, is the passband frequency, 2.0 Hz.
7. In this example for a highpass filter we enter 30 Hz, the sampling frequency.
8. For lowpass or highpass filter:
   either enter stop-band frequency as a positive number in Hz or
   enter stop-band ripple as a negative number in dB.
   For band-pass or band-stop filter:
   enter stop-band ripple as a negative number in dB.
   In this example of highpass filter, we enter stop-band frequency +1.7 Hz.

PROGRAM LLITG:

1. Enter name of output file from program IRR which contains the filter coefficients - FILTER.DAT in this example.
2. Number of data points in the acceleration time history -

1024 in this example.

3. Sampling frequency in Hz - 30 Hz in this example.
4. C8031.RO3 is an example input acceleration BINARY data file name.
5. C8031.DO3 is an example output displacement BINARY data file name.

The displacement figures shown in this thesis were obtained from double integration of 1500 (50 sec) acceleration data points. Because of the transient effect of the filters (also integrators) on the beginning and ending parts of the data, 238 data points were discarded on both ends and a total of 1024 (34.14 sec) displacement data points were shown in those figures.

Program LLITG can integrate at most 2048 data points. For the 2 1/2 hour long records, as shown in Figures 25 through 28, modification of this program was required. The program was broken into individual steps as described in Chapter 3, section 5. In each step, the data was processed segment by segment. Because of the transient effect in the filters (also integrators), each segment was not processed independently of the next segment. Careful linkage between segments was done by storing the ending of the previous segment, and using it as the beginning of the next segment, so that transients were eliminated in moving from one segment to the next.